



**HAL**  
open science

## Theoretical electroelastic moduli of porous textured piezoceramics

Antoine Balé, Rémi Rouffaud, F. Levassort, Anne-Christine Hladky, Pascal Marchet

► **To cite this version:**

Antoine Balé, Rémi Rouffaud, F. Levassort, Anne-Christine Hladky, Pascal Marchet. Theoretical electroelastic moduli of porous textured piezoceramics. IEEE international Ultrasonics Symposium 2018, Oct 2018, Kobe, Japan. 10.1109/ultsym.2018.8579661 . hal-02142064

**HAL Id: hal-02142064**

**<https://unilim.hal.science/hal-02142064v1>**

Submitted on 24 Sep 2019

**HAL** is a multi-disciplinary open access archive for the deposit and dissemination of scientific research documents, whether they are published or not. The documents may come from teaching and research institutions in France or abroad, or from public or private research centers.

L'archive ouverte pluridisciplinaire **HAL**, est destinée au dépôt et à la diffusion de documents scientifiques de niveau recherche, publiés ou non, émanant des établissements d'enseignement et de recherche français ou étrangers, des laboratoires publics ou privés.

# Theoretical Electroelastic Moduli of Porous Textured Piezoceramics

Antoine Balé, Rémi Rouffaud,  
Franck Levassort  
GREMAN, University of Tours, CNRS, INSA CVL  
Tours, France  
antoine.bale@univ-tours.fr

Anne-Christine Hladky-Hennion  
ISEN dept., IEMN, CNRS  
Lille, France  
anne-christine.hladky@isen.fr

Pascal Marchet  
IRCER, University of Limoges, CNRS  
Limoges, France  
pascal.marchet@unilim.fr

**Abstract**—Nowadays, piezoceramics are commonly used in ultrasonic transducers (underwater applications, medical imaging, NDT...). Most of them are PZT-based materials ( $\text{Pb}(\text{Zr,Ti})\text{O}_3$ ), which causes environmental issues due to the presence of lead. To comply with international regulations on the use of lead, numerous studies are conducted on lead-free piezoceramics ( $\text{K}_{0.5}\text{Na}_{0.5}\text{NbO}_3$ ,  $\text{BaTiO}_3$ ) which can offer similar electromechanical performance to lead-based materials. Fabrication of lead-free textured ceramics enables the production of large area of piezoelectric materials with good electromechanical capabilities. Textured ceramics can be simply modeled as a 3-phases composite: one for the single-crystal that increases with the texturation degree, another one for the ceramic matrix and a last one for porosity. The amount of porosity depends on the sintering conditions. In the long wavelength approximation, this material can be considered as homogeneous and characterized by effective properties. In this context, few studies were carried out for this homogenization step and, in this paper, a homogenization scheme is developed, based on the generalization of series and parallel connections. For the modeling, a unit cell is defined and used to determine the effective electroelastic moduli. Then, a validation step for this model is performed using FEM calculation. Results show that a high texturation is necessary and that the presence of porosity is not always damaging to optimize the targeted performance. Finally, theoretical properties of two single-element transducers based on textured piezoceramics are determined and compared to those based on PZT.

**Index Terms**—homogenization, modeling, piezoelectricity, porosity, textured ceramics

## I. INTRODUCTION

Although piezoelectric single-crystals have high electromechanical properties, their use is limited for various applications because of their low mechanical resistance, their time-consuming production and their shape/size limitations. In order to avoid these problems, a trade-off can be found with textured ceramics. Indeed, grain orientation can lead to higher piezoelectric properties than those of conventional ceramics with the same composition. By this way, single-crystal like properties can be attained.

Because of the complex structure of textured ceramic, there are only few models on effective properties: Li [3] proposed a calculation scheme based on a self-consistent approach to

determine the full effective electroelastic moduli of textured  $\text{BaTiO}_3$  polycrystalline aggregates. Uniaxial texture was considered and incorporated using an orientation distribution function assumed to be a Gaussian distribution. Several authors have developed models based on self-consistent approach too [4], [5]. Jayachandran *et al.* [6] used the Finite Element Method (FEM) to model textured ceramics. The modelling is performed at the microscopic scale, which allows authors to define accurate orientations. They studied the effect of texturation on the effective properties of different materials as  $\text{BaTiO}_3$  (BT),  $\text{PbTiO}_3$  (PT) or PMN-24PT. Moreover, thanks to the FEM, they can take into account the porosity or damages from the fabrication process.

While several studies have acknowledged that a high porosity content degrades the piezoelectric and dielectric properties of materials, they have also demonstrated an overall increase in the figure of merit values, such as  $d_h g_h$  for hydrophone applications or the electromechanical coupling factor  $k_t$  for medical ultrasonics and underwater applications [7], [8]. Furthermore, when considering specific transducer applications, porosity allows for a decrease in acoustical impedance, which in turn allows for a better transfer of acoustical energy to water and biological tissue.

Using similar models, the influence of the porosity in piezoceramics considered to be 2-phase composites (pores and piezoelectric materials) are also quantified. Numerous

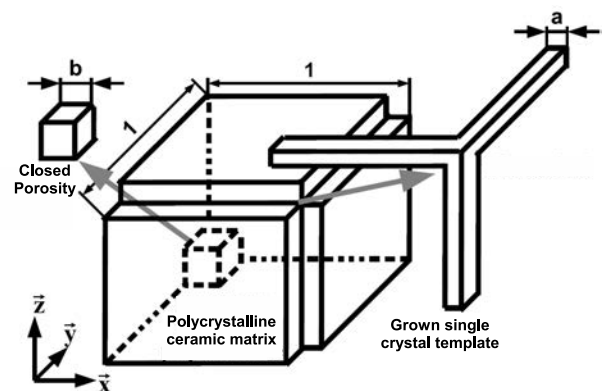


Fig. 1. Definition of the unit cell for porous textured ceramics.

TABLE I  
ROOM-TEMPERATURE ELASTIC STIFFNESS  $c^E$  (IN  $10^{10}$  PA), PIEZOELECTRIC COEFFICIENT  $e$  (IN C/M<sup>2</sup>), DIELECTRIC CONSTANT AT CONSTANT STRAIN  $\epsilon^S/\epsilon_0$ , THICKNESS COUPLING FACTOR  $k_t$  AND DENSITY (IN KG/M<sup>3</sup>) OF PMN-33PT SINGLE-CRYSTAL AND PMN-34,5PT CERAMIC.

Parameters	$c_{11}^E$	$c_{12}^E$	$c_{13}^E$	$c_{33}^E$	$c_{44}^E$	$c_{66}^E$	$e_{15}$	$e_{31}$	$e_{33}$	$\epsilon_{11}^S/\epsilon_0$	$\epsilon_{33}^S/\epsilon_0$	$k_t$	$\rho$
PMN-33PT [1]	11.5	10.3	10.2	10.3	6.9	6.6	10.1	-3.9	20.3	1434	680	0.64	8060
PMN-34.5PT [2]	17.5	11.7	11.9	15.5	2.7	2.9	17.1	-6.4	27.3	2373	2825	0.4	8060

other approaches have been considered, such as the FEM, the self-consistent scheme, percolation, and fractal analysis. Readers are referred to Rybyanets's review article on porous piezoceramics for further details [9].

In this study, we propose modeling textured ceramics while taking the porosity content into account. In this case, a new unit cell comprised of three phases (single crystal, ceramic, and porosity) will be used. The calculation scheme makes use of the interfacial boundary conditions, which allows for determining all piezoelectric, elastic, and dielectric properties of the composite. The final objective is to quantify the effect of texturation and porosity on some figures of merit like the thickness coupling coefficient  $k_t$ .

First, we describe the implemented model and the choice of the unit cell. The validation of the model is performed with FE calculations. Then, theoretical results for the thickness mode of a PMN-PT-based material are presented. Lastly, the electroacoustic response of one single-element transducer is simulated with the porous textured ceramic and compared with different standard configurations.

## II. MODEL DESCRIPTION

The Template Grain Growth (TGG) method enables the fabrication of highly textured ceramics with an enhanced piezoelectric response [10]. When sintered at high temperatures, single-crystal oriented templates grow at the expense of the finer matrix grains. When the process is finished, the microstructure can be regarded as large areas of grown templates that can be in contact with one another and randomly distributed in the residual matrix. Furthermore, porosity can also be present in the residual matrix. This description can be translated into a representative unit cell.

### A. Unit Cell

To describe the spatial arrangement of the several phases using the previously described microstructure, the concept of connectivity [11] can be used and extended to textured ceramics considering two piezoelectric phases. The oriented phase is self-connected in three dimensions in the residual matrix (same consideration for this second phase) and a 3-3 connectivity defines this material. Moreover, in taking the closed porosity into account, the 3-(0-3) connectivity is retained for the entire material. The exploded view of the unit cell is shown on Fig.1.

The textured ceramic is regarded as a composite made up of two piezoelectric phases as well as a porosity phase and

is represented by a unit cubic cell. Both inclusions in the unit cell are defined by two independent variables  $a$  and  $b$ ;  $a$  specifies additional dimensions of the 3-3 inhomogeneity (single-crystal) and  $b$  specifies the dimensions of the 0-3 inhomogeneity (pores) (Fig.1).

From this representation, a simple decomposition of the unit cell in a 2-2 or 1-3 connectivity is not possible due to a compactness limit [12]. Indeed, if  $b = 1 - a$ , both corresponding inclusions are in contact but do not fill the whole unit volume of the cell and the total volume fraction does not reach 1, hence the use of the "composite of composites" approach, where the unit cell used to describe the material is viewed as a 3-3 composite in which the polycrystalline matrix and the closed porosity is considered a 0-3 composite.

This approach requires calculating an intermediate effective 0-3 modulus  $[K]_{0-3}$  before being able to calculate the final effective matrix  $[K]$  of the homogenized material. To homogenize the 0-3 composite, an intermediate non-unit cubic cell, which excludes the interconnected single crystal, has a total volume of  $V_{0-3} = 1 - 3a^2 + 2a^3$ . To calculate the effective parameters, the 0-3 cell is split into two blocks with a two-step process required. The first step consists of homogenizing the 2-2 series connectivity (porosity + polycrystalline ceramic) using the volume fraction:

$$v_1 = \frac{b}{(1 - 3a^2 + 2a^3)^{1/3}} \quad (1)$$

Finally, the intermediate  $[K]_{0-3}$  matrix is determined by assembling the last two blocks [12] in a 1-3 connectivity using the volumic fraction:

$$v_2 = \frac{b^2}{(1 - 3a^2 + 2a^3)^{2/3}} \quad (2)$$

The three-step homogenization process for the 3-3 connectivity can be performed. The new cell, which contains the 3-3 single-crystal connectivity and the effective medium matrix with 0-3 properties ( $[K]_{0-3}$ ), is broken up into four blocks as detailed in [12]. The first step consists in homogenizing the 2-2 series connectivity. These blocks are then assembled into a 1-3 connectivity with the block containing the intermediate effective medium. Finally, the block with the vertical branch of the single-crystal inclusion is also assembled into a 1-3 connectivity with the rest of the cell and the final effective matrix  $[K]$  of the composite is obtained.

TABLE II  
COMPARISON OF THE ELECTROMECHANICAL COUPLING FACTOR  $k_t$  AS A FUNCTION OF THE POROSITY VOLUME FRACTION OBTAINED BY THE DESCRIBED MODEL AND BY THE FEM FOR A 50% VOLUME FRACTION OF A SINGLE-CRYSTAL.

porosity (%)	0	1	2	3	4	5	6	7	8	9	10	11	12,5
$k_t$ (% FEM)	50.3	50.7	52.3	52.6	53.4	54.2	55.2	55.9	56.5	57.4	58	59	59.5
$k_t$ (% current model)	50.7	51.8	52.5	53.4	54.1	54.8	55.5	56.2	56.9	57.5	58.2	58.8	59.8

### B. Validation

For the matrix method calculation, a PMN-PT-based material was selected. Templates (single-crystal) and ceramic matrix are of similar compositions. PMN-33PT [1] was chosen as the single-crystal phase and PMN-34.5PT [2] as the ceramic. Full data sets are presented in Table I.

To corroborate the results obtained by the described model, finite element parametric study was performed using the same cubic unit cell defined in Fig.1. To prioritize the thickness mode through a harmonic analysis, a simulation of piston-like behavior was needed. To achieve this, meshing was performed on 5 unit cells stacked on top of one another. Calculations were performed with the ATILA software [13].

The resulting resonance ( $f_r$ ) and antiresonance ( $f_a$ ) frequencies (FEM calculations) are obtained through impedance curves and range from 150 to 250 kHz. The thickness coupling coefficient  $k_t$  is evaluated using the resonance/antiresonance frequencies formula:

$$k_t^2 = \frac{\pi f_r}{2 f_a} \tan\left(\frac{\pi f_a - f_r}{2 f_a}\right) \quad (3)$$

while the standard static formula is used to evaluate the  $k_t$  using results obtained by the matrix method:

$$k_t^2 = \frac{e_{33}^2}{c_{33}^D \epsilon_{33}^S} \quad (4)$$

A comparison of the thickness coupling coefficient as a function of the porosity content obtained by both methods for a 50% single-crystal volume fraction is presented in Table

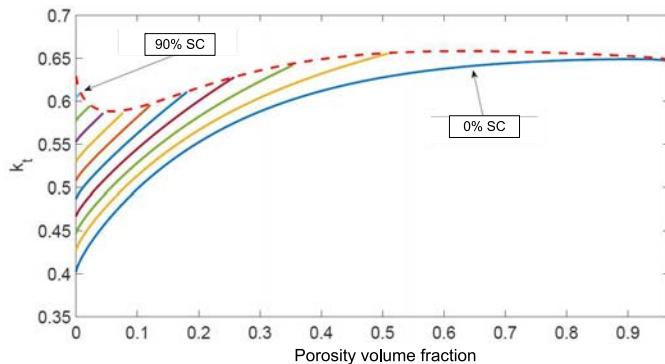


Fig. 2. Variations of coupling coefficient  $k_t$  as a function of porosity content. Solid lines represent different SC volume fractions from 0% to 90% by a 10% step.

II. First, the maximum porosity content attainable (0.13) for this single-crystal volume fraction is restricted by the choice of unit cell, particularly the shape and dimensions of both inclusions (compactness limit). The results from both methods are in good agreement and the largest differences (lower than 1%) can be explained by the method used to determine the  $k_t$  values [14].

### III. RESULTS

Now that the validation is done, one can quantify the effect of the porosity on the electromechanical behavior of the textured ceramic. The coupling coefficient  $k_t$  is calculated as a function of porosity content. Then, simulation of single-element transducer including the porous textured ceramic is performed with the most advantageous value of porosity. The same materials data as the validation step are used.

#### A. Coupling coefficient

Fig.2 represents the electromechanical coupling factor  $k_t$  as a function of the porosity volume fractions for the previously studied PMN-PT system. The red dashed line corresponds to the limiting condition on the dimensions of both inclusions previously mentioned. The coupling coefficient values for a pure ceramic phase and pure single-crystal phase are located at 0% porosity volume fraction on the 0% SC curve and on the 100% SC curve, respectively. One can notice that the porosity volume fraction of 1 is omitted as the  $k_t$  value is nul. Furthermore, results for porosity content over 25% should be treated with caution as these configurations cannot be realistically implemented in transducers due to low mechanical resistance.

On Fig.2,  $k_t$  increases with the increase of porosity for a

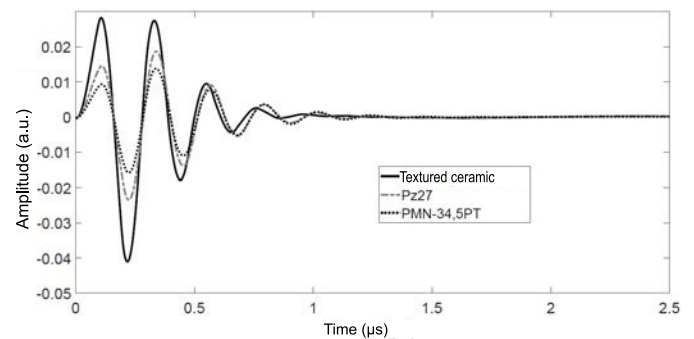


Fig. 3. Electroacoustic responses (arbitrary unity) in water for 3 single-element transducers.

constant SC volume fraction. In the same way, for a constant porosity volume fraction, the coupling coefficient increases with the rise of SC. In order to simulate the single-element transducer, the porous textured ceramic with 70% SC and 4.4% of porosity is selected because of its high  $k_t$  (58.6%).

### B. Single-element transducer

In order to highlight performance of the selected porous textured ceramic, electroacoustic responses of single-element transducer are performed. A backing with an acoustic impedance of 15 MRa is chosen with a Ø10mm disk of porous textured ceramic. The center frequency is chosen at 4.5MHz and material thickness is modified accordingly. The simulation of transducer electro-acoustic responses (without matching layer) is performed in water and based on equivalent electrical scheme KLM [15].

With the same parameters, simulations with PMN-34.5PT [2] and Pz27 [12] ceramics, and PMN-33PT [1] SC are performed. Electroacoustic responses are calculated and only 3 of them are presented on fig.3 not to overload the graph. Sensitivities and -6dB relative bandwidth are summarized in table III. One can notice a +7.5dB increase for the sensitivity of the porous textured ceramic-based transducer by comparison with the PMN-34.5PT ceramic. Nevertheless, its efficiency is slightly lower than that of the PMN-33PT. Finally, a simulation is done with Pz27 [16] as it is a common soft PZT material for these applications. Pz27's sensitivity is 2.5 times lower than that of the textured ceramic. A relative difference for the bandwidth of +20% and +15% are obtained in comparison to PMN-34.5PT and Pz27, respectively.

TABLE III  
NORMALIZED SENSITIVITIES IN RELATION TO THE PMN-34.5PT SENSITIVITY AND -6dB RELATIVE BANDWIDTH ( $BW_{-6dB}$  IN %).

	PMN-34.5PT	Pz27	Textured ceramic	PMN-33PT (SC)
Sens. (dB)	0	+3	+7,5	+8,9
$BW_{-6dB}$	37,6	43	57	58

### IV. CONCLUSION

A matrix method, which was previously applied to piezoelectric composites with various connectivities, was extended to porous, textured ceramics, and within the long wavelength approximation, the effective electroelastic moduli of the materials were deduced. The results and discussion mainly focus on the thickness parameters and, in particular, the electromechanical thickness coupling factor  $k_t$ . The results showed that an improvement of the electromechanical coupling coefficient can be achieved in two ways: a high texturing of the ceramic with limited porosity content or a lower degree of texture coupled with an increased porosity volume fraction.

Some limitations can be recalled such as the use of an ideal

structure where the SC phase has a perfect orientation or the fact that only a closed porosity was taken into account.

### ACKNOWLEDGMENT

This work was supported by the French Research Agency (HEcATE project ANR 14-CE07-0028-01).

### REFERENCES

- [1] R. Zhang, B. Jiang, and W. Cao, "Elastic, piezoelectric, and dielectric properties of multidomain  $0.67\text{Pb}(\text{Mg}_{1/3}\text{Nb}_{2/3})\text{O}_3-0.33\text{PbTiO}_3$  single crystals," *Journal of Applied Physics*, vol. 90, no. 7, pp. 3471–3475, oct 2001. [Online]. Available: <http://aip.scitation.org/doi/10.1063/1.1390494>
- [2] T. Delaunay, "Caractérisation fonctionnelle et relations structure-propriétés de monocristaux piézoélectriques de type pérovskite," Ph.D. dissertation, Université François-Rabelais, Tours, France, [in french] 2006.
- [3] J. Yu Li, "Effective electroelastic moduli of textured piezoelectric polycrystalline aggregates," *Journal of the Mechanics and Physics of Solids*, vol. 48, no. 3, pp. 529–552, 2000.
- [4] V. I. Aleshin, I. P. Raevskii, and E. I. Sitalo, "Electromechanical properties of a textured ceramic material in the (1 - x)PMN-xPT system: Simulation based on the effective-medium method," *Physics of the Solid State*, vol. 50, no. 11, pp. 2150–2156, 2008.
- [5] J. Ruglovsky, J. Li, B. Kaushik, and A. H. Atwater, "The Effect of Biaxial texture on the Effective Electrochemical Constants of Polycrystalline Barium Titanate and Lead Titanate Thin Films," *Acta Materialia*, vol. 54, pp. 3657–3663, 2006.
- [6] K. P. Jayachandran, J. M. Guedes, and H. C. Rodrigues, "Homogenization of textured as well as randomly oriented ferroelectric polycrystals," *Computational Materials Science*, vol. 45, no. 3, pp. 816–820, 2009.
- [7] H. Kara, R. Ramesh, R. Stevens, and C. R. Bowen, "Porous PZT ceramics for receiving transducers," *IEEE Transactions on Ultrasonics, Ferroelectrics, and Frequency Control*, vol. 50, no. 3, pp. 289–296, 2003.
- [8] F. Levassort, J. Holc, E. Ringgaard, T. Bove, M. Kosec, and M. Lethiecq, "Fabrication, modelling and use of porous ceramics for ultrasonic transducer applications," *Journal of Electroceramics*, vol. 19, pp. 125–137, 2007.
- [9] A. N. Rybyanets, "Porous Piezoceramics : Theory, Technology, and Properties," *IEEE transactions on ultrasonics, ferroelectrics, and frequency control*, vol. 58, no. 7, pp. 1492–1507, 2011.
- [10] G. L. Messing, S. Trolrier-McKinstry, E. M. Sabolsky, C. Duran, S. Kwon, B. Brahmaraoutu, P. Park, H. Yilmaz, P. W. Rehrig, K. B. Eitel, E. Suvaci, M. Seabaugh, and K. S. Oh, "Templated grain growth of textured piezoelectric ceramics," *Critical Reviews in Solid State and Materials Sciences*, vol. 29, no. 2, pp. 37–41, 2004.
- [11] R. E. Newnham, D. P. Skinner, and L. E. Cross, "Connectivity and Piezoelectric-Pyroelectric Composites," *Material Research Bulletin*, vol. 13, no. 5, pp. 525–536, 1978.
- [12] F. Levassort, M. Lethiecq, R. Desmare, and L. P. Tran-Huu-Hue, "Effective electroelastic moduli of 3-3(0-3) piezocomposites," *IEEE Transactions on Ultrasonics, Ferroelectrics, and Frequency Control*, vol. 46, no. 4, pp. 1028–1034, 1999.
- [13] "ATILA, Finite-Element Software Package for the analysis of 2D & 3D structures based on smart materials," 2010.
- [14] S. H. Chang, C. C. Chou, and N. N. Rogacheva, "Analysis of Methods for Determining Electromechanical Coupling Coefficients of Piezoelectric Elements," *IEEE Transactions on Ultrasonics, Ferroelectrics, and Frequency Control*, vol. 42, no. 4, pp. 630–640, 1995.
- [15] R. Krimholtz, D. A. Leedom, and G. L. Matthaei, "New equivalent circuits for elementary piezoelectric transducers," *Electronics Letters*, vol. 6, no. 13, p. 398, 1970. [Online]. Available: [http://digital-library.theiet.org/content/journals/10.1049/el\\_19700280](http://digital-library.theiet.org/content/journals/10.1049/el_19700280)
- [16] MEGGITT Ferroperm. [Online]. Available: <https://www.meggittferroperm.com/>